ELSEVIER

1 February 1997

OPTICS COMMUNICATIONS

Optics Communications 135 (1997) 138–148

Full length article

Reflection cooling of sodium atoms in an evanescent light wave

D.V. Laryushin, Yu.B. Ovchinnikov [1], V.I. Balykin, V.S. Letokhov

Institute of Spectroscopy, Russian Academy of Sciences, 142092 Troitsk, Moscow Region, Russia

Received 8 May 1996; accepted 19 September 1996

Abstract

Studied in this work is the cooling of a beam of sodium atoms upon its reflection from an evanescent light wave. The cooling mechanism is associated with the spontaneous transitions of the atoms between the hyperfine-structure sublevels of the ground state. Subject to studies is the relationship between the reflection angle of the atoms and the frequency detuning and intensity of the light wave. It is demonstrated experimentally that the transverse atomic momentum component can be reduced by more than one half ($\Delta p_\perp / p_\perp \cong 0.5$) in a single reflection event, the number of cooled atoms in the reflected beam exceeding 50%. It should be noted that the loss of atoms in reflection can be made as small as desired, and so the reflection cooling cycle can be repeated many times over.

PACS: 32.80.Pj

1. Introduction

Laser radiation is an effective means of cooling atoms by extracting from their translational energy [1,2]. The withdrawal of energy from an atom results from its inelastic scattering of laser photons. In that case, for the total energy of the "laser field + atom" system to be conserved, it is necessary that the scattered photons have shorter-wavelength than the initial laser field photons.

There are several methods of implementing this laser cooling principle. The first of these methods (Doppler cooling) [3,4] uses the Doppler shift of the resonance frequency of the atom. On average, the atom in each photon scattering cycle will lose an energy of $\Delta E \approx \hbar k v$ proportional to its velocity v, where k is the wave vector. The minimum temperature to which atoms can be cooled by the Doppler cooling method is $T_D = \hbar\gamma / k_B$ [5] (the so-called Doppler limit), where k_B is the Boltzmann constant.

The second atomic cooling mechanism ("retarded force cooling") [6,7] is based on the light-induced shifting of the energy levels in the atom and nonadiabatic evolution of its internal state in the course of movement in a spatially inhomogeneous light field. The energy of a two-level atom in this case changes by the "quanta" $\Delta E \approx A^2(d_{12}^2/4\hbar\delta)$ equal to the light-induced shift of the atomic energy levels, A being the amplitude of the light field, d_{12} the dipole transition matrix element, and δ the detuning of the light field frequency with respect to the resonance transition frequency. Since the energy of such a "quantum" being high, the rate of such cooling in intense light fields may substantially exceed the Doppler cooling rate [8]. However, the minimum temperature of the two-level atoms cooled in this way remains above the Doppler limit.

The "Sisyphus cooling" method [9] uses the superposition of standing light waves differing in polarization, which gives rise to spatially modulated light-induced shifts of magnetic sublevels in the atom. The Sisyphus cooling of the atom occurs as a result of being optically pumped between these sublevels. Where the light field intensity is low, so that the time it takes for the atom to be pumped between the sublevels is long, $\tau \gg 2\gamma$, and the light-induced shift is small, $\Delta\omega \ll \gamma$, the ultimate temperature of the cooled atoms may be considerably lower than the Doppler limit.

The authors of Ref. [10] have suggested another version of the Sisyphus cooling method. Use is made here of the

[1] Present address: Max-Plank-Institut für Kernphysik, 69029 Heidelberg, Germany.

PII S0030-4018(96)00610-4

optical pumping of an alkali metal atom between the hyperfine structure sublevels of its ground state in a bichromatic standing light wave. In its principle and capabilities, this method is closely similar to the polarization cooling technique. A specific feature of the Sisyphus cooling in a standing light wave is the narrow atomic velocity variation range at fixed light field parameters.

The authors of Ref. [11] have proposed a method for cooling alkali metal atoms, which uses spontaneous transitions between the hyperfine structure sublevels of the ground state in an evanescent light wave. This method combines the advantages of the retarded force cooling (large cooling quantum) and the Sisyphus cooling (low ultimate temperature of the cooled atoms). This cooling mechanism has already been discussed by Helmerson et al. [12]. The atom loses energy upon reflection from the evanescent wave. The energy quantum withdrawn from the atom is equal to the difference between the light-induced shifts of the hyperfine structure sublevels of the ground atomic state at the point of spontaneous transition between these sublevels. This difference increases as the atom approaches the dielectric-vacuum interface and the intensity of the evanescent light wave becomes higher. The penetration depth of the atom into the evanescent wave being proportional to its kinetic energy, the energy quantum extracted from the atom decreases as it gets colder. This makes it possible to rapidly cool atoms from high initial kinetic energies to sub-Doppler temperatures $T \approx \hbar^2 k^2 / 2Mk_B$ corresponding to an atomic momentum of a few $\hbar k$ units [13].

We were the first to observe experimentally this cooling mechanism for a thermal beam of sodium atoms reflecting once from an evanescent light wave [14]. In this paper, we present the results of detailed experimental study into the cooling of atoms in an evanescent light wave, including the relationships between the cooling effect and the frequency detuning and intensity of the light field.

2. Mechanism of atomic cooling in an evanescent wave

The evanescent-wave-based mirror for neutral atoms was proposed by Cook and Hill [15] and has since been used effectively for both thermal beams [16] and cold atoms [17,18]. The mechanism of atomic reflection from such a mirror was described in detail, for example, in Ref. [18], and so we will only briefly recall here the main characteristics of the atomic mirror.

When a Gaussian light beam undergoes total internal reflection at a dielectric-vacuum interface, an evanescent wave is formed in the vacuum (Fig. 1), whose amplitude decays exponentially as

$$A(x, z) = A_0 \exp\left[-z/\Lambda - (x/w_x)^2 - (y/w_y)^2 - \mathrm{i}k_x x\right], \quad (1)$$

where x and z are the coordinates parallel with and perpendicular to the interface, respectively, $w_x = w/\cos\theta_i$, $w_y = w$ are the Gaussian beam waists in the x- and y-directions, Λ is the characteristic wave decay length in the vacuum given by

$$\Lambda = (\lambda/2\pi)\left(n^2 \sin\theta_i - 1\right)^{-1/2}, \quad (2)$$

n is the refractive index of the dielectric, and θ_i is the angle of incidence of the light beam. The evanescent wave propagates over the interface with the wave vector

$$k_x = (2\pi/\lambda) n \sin\theta_i. \quad (3)$$

The Rabi frequency in such a light field depends exponentially on the z-coordinate as

$$\Omega_R(z) = \Omega_R(0) \exp(-z/\Lambda), \quad (4)$$

where $\Omega_R(0)$ is the Rabi frequency at the dielectric–vacuum interface.

The dressed states method [7] is the most convenient way to describe the motion of an atom in a strong light field. For a two-level atom, the eigenvalues of the dressed states are

$$U_{n,\pm}(z) = (n+1)\hbar\omega - \tfrac{1}{2}\hbar\Delta \pm \tfrac{1}{2}\hbar\Omega(z), \quad (5)$$

where n is the number of the light-field photons, $\Delta = \omega - \omega_0$ is the detuning of the light-field frequency off resonance with the atomic transition frequency, and $\Omega(z) = (\Omega_R^2(z) + \Delta^2)^{1/2}$ is the effective Rabi frequency. In the case of positive frequency detuning, the initial state consisting of an atom in the ground state and $n+1$ photons evolves adiabatically into the dressed state $|+, n\rangle$ wherein the atom is repelled out of the light field. The overall dynamics of an atom is governed by the dressed states along which it propagates and the spontaneous transitions it makes between them. In each spontaneous emission event, the atom not only changes its dressed state, but also acquires an additional recoil momentum of $\hbar k$.

Consider a typical situation for alkali atoms. Fig. 2a presents the energy level diagram of the D_2 line of the sodium atom and shows the position of the evanescent light wave frequency ω exceeding by an amount of δ the frequency of the atomic transition between the sublevel $|F=1\rangle$ of the ground state and the excited state $|e\rangle$. The principal simplification of this diagram is that the excited state $3^2P_{3/2}$ is treated without considering its hyperfine structure with the characteristic distance between sublevels amounting to $\delta_e/2\pi = 50$ MHz, which is justified at $\delta \gg \delta_e$. In the light wave, the states $|F=1, n+1\rangle$, $|F=2, n+1\rangle$, and $|e\rangle$ form a triplet of the dressed states $|1, n\rangle$, $|2, n\rangle$, and $|3, n\rangle$ (Fig. 2b).

In the first-order perturbation theory approximation, the individual light-induced shift of each magnetic sublevel (F, m) of the ground state is a sum of the contributions from all the allowed π-transitions $(F, m) \rightarrow (F', m)$:

$$U_{Fm} = (2J'+1)\frac{\hbar}{2}\sum_{F'}\left(\sqrt{\Omega_{Fm,F'm}^2 + \delta_{FF'}^2} - \delta_{FF'}\right), \quad (6)$$

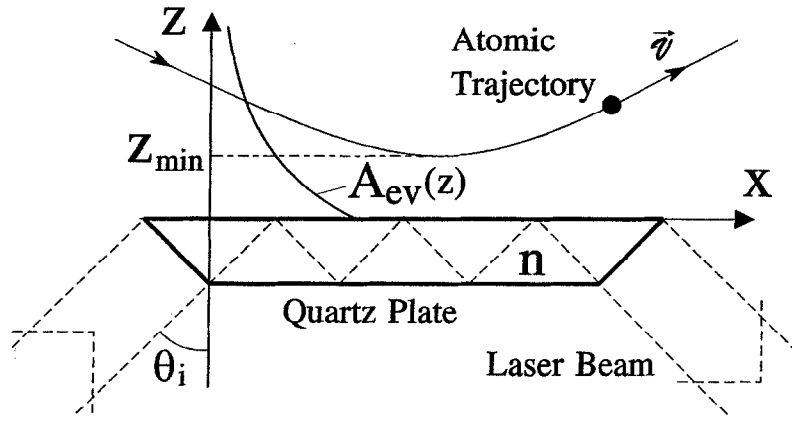

Fig. 1. Schematic diagram of the atomic mirror. The laser beam is brought at an angle of $\theta = 45°$ into a quartz plate and produces on its surface an evanescent light wave with an exponentially decaying amplitude $A(z)$.

where $\Omega_{Fm,F'm}$ and $\delta_{FF'}$ are the Rabi frequency and laser frequency detuning of the transition, respectively. In the case of large frequency detuning values, $\delta \gg \delta_e$ and $\delta > \Omega_{Fm,F'm}$ one can obtain optical potential expressions for both the hyperfine-structure sublevels:

$$U_1(z) = \frac{\hbar}{2}\left(\sqrt{(2/3)\Omega_R^2 + \delta^2} - \delta\right), \tag{7a}$$

$$U_2(z) = \frac{\hbar}{2}\left(\sqrt{(2/3)\Omega_R^2 + (\delta_{hfs} + \delta)^2} - \delta_{hfs} - \delta\right), \tag{7b}$$

where $\Omega_R = \Gamma(I_{ev}/2I_{sat})^{1/2}$ is the effective Rabi frequency of a two-level atom with a spontaneous decay rate of Γ. Note that the optical potential barrier height for an atom residing at the $|F = 2\rangle$ sublevel is much lower than that for an atom at the sublevel $|F = 1\rangle$, thanks to the greater frequency detuning $\delta + \delta_{hfs}$. The above expressions (7a) and (7b) for the optical potentials are similar to the corresponding expressions for the two-level atom at the corresponding frequency detuning values, except for the factor 2/3 which appears when extending summation over all the possible transitions to the hyperfine-structure sublevels of the excited state.

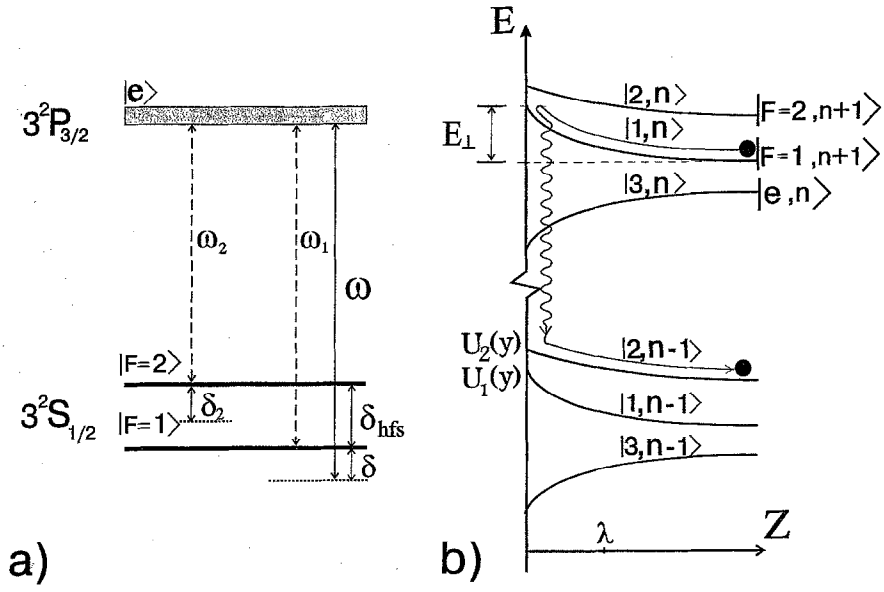

Fig. 2. (a) Schematic diagram of the hyperfine splitting of the D_2 transition of the sodium atom (dashed arrows). The solid arrow indicates the position of the evanescent wave laser frequency. (b) Energy level diagram of the dressed sodium atom. The mechanism of atomic cooling in the evanescent wave is as follows. The atom enters the light field while residing at the lower sublevel $|F = 1\rangle$ of its ground state and is retarded in the potential $U_1(z)$. Having undergone the spontaneous decay to the sublevel $|F = 2\rangle$, the atom finds itself in the less repelling potential $U_2(z)$ and will be unable to reach its initial velocity upon acceleration.

Let the atom reside initially at the sublevel $|F=1\rangle$ and have a kinetic energy

$$E_\perp = Mv_\perp^2/2 < U_1(0), U_2(0), \tag{8}$$

outside the evanescent wave, where $v_\perp$ is the atomic velocity component normal to the surface of the atomic mirror. In that case, in the absence of spontaneous decays, the atom is reflected elastically from the potential U_1. When spontaneous decays are present, the atom may transit from the dressed state $|1, n\rangle$ to one of the states $|i, n-1\rangle$ (Fig. 2b). The transition rates for the case of weak saturation, $\Omega_R^2/2\delta^2 \ll 1$, were presented in Ref. [13]. In our experiment, the optimum frequency detuning was of the order of the Rabi frequency and substantially less than the distance between the sublevels $|F=1\rangle$ and $|F=2\rangle$ of the ground state. In this approximation, the transition rates have the form

$$\Gamma_{11} = q\frac{\Gamma}{4}\frac{(2/3)\Omega_R^2}{\delta^2+(2/3)\Omega_R^2}, \tag{9a}$$

$$\Gamma_{12} = (1-q)\frac{\Gamma}{4}\frac{(2/3)\Omega_R^2}{\delta^2+(2/3)\Omega_R^2}, \tag{9b}$$

$$\Gamma_{13} = \frac{\Gamma}{4}\left(1-\frac{\delta}{\sqrt{\delta^2+(2/3)\Omega_R^2}}\right)^2, \tag{9c}$$

where $q=0.72$ is the mean branching ratio to the lower hyperfine ground state for the scattering of an evanescent wave photon.

As a result of the $|1, n\rangle \to |2, n\rangle$ transition, the atom ends up in a lower potential and loses some potential energy, $U_1(z_{1\to 2}) - U_2(z_{1\to 2}) > 0$, where $z_{1\to 2}$ is the distance from the surface at which the spontaneous transition has occurred. Graphically speaking, the atom climbs up a high mountain, but comes down a small hill. The average kinetic energy loss per reflection event resulting from such a Sisyphus cooling is

$$\langle \Delta E_\perp \rangle = \int_{-\infty}^{\infty} (U_1 - U_2) p_1(t) \Gamma_{12}\, dt \approx \frac{2}{3}\frac{\delta_{hfs}}{\delta+\delta_{hfs}} E_\perp p_{12}, \tag{10}$$

where $p_1(t) = \exp[-\int_{-\infty}^{t}\Gamma_{12}(\zeta)\,d\zeta]$ is the probability that the atom will remain in the state $|1, n\rangle$ at the instant t. The probability that the atom will reflect inelastically from the evanescent wave as a result of being pumped to the upper sublevel of the ground state is

$$p_{12} = 1 - \exp\left(-\int_{-\infty}^{\infty}\Gamma_{12}(t)\,dt\right) \approx (1-q)\frac{m\Lambda\Gamma}{\hbar\delta}v_\perp. \tag{11}$$

The quantities $\langle \Delta E_\perp \rangle$ and p_{12} determine the efficiency of cooling of the atomic beam upon its reflection from the evanescent wave. It follows from expression (10) that as the frequency detuning δ is reduced, the loss of the transverse momentum component by the atom experiencing the decay $|1, n\rangle \to |2, n-1\rangle$ increases. In that case, inelastic reflection probability (11) becomes higher, which leads to an increase of the number of cooled atoms in the reflected beam. However, as the frequency detuning is reduced to fall within the region ($\delta < \Omega_R$), the decays to the attractive state $|3, n-1\rangle$ become important and this results in heating of the atoms. In our experiment, the deepest cooling of the atomic beam was achieved at a frequency detuning of $\delta \approx \Omega_R(z_{min})$, where z_{min} is the minimum distance between the atom and the dielectric surface.

3. Experiment

The idea to measure the cooling of atoms upon their reflection was mainly as follows. A thermal beam of sodium atoms was incident at a small angle on the surface of a quartz plate (Fig. 3) along which an evanescent light wave was propagating. To observe the cooling effect, the atoms in the beam were preliminarily pumped optically to the sublevel $|F=1\rangle$. While reflecting, some atoms in the incident beam experienced spontaneous decays to the sublevel $|F=2\rangle$. The decrease of the transverse kinetic energy component of such atoms, defined by formula (10), resulted in that their angle of reflection proved smaller than in the case of specular reflection. Thus, using the selective detection of the atoms residing at the sublevel $|F=2\rangle$, we observed a reflected beam profile shift towards smaller angles of reflection. The specular angle of reflection was determined by observing the reflection of a beam of atoms initially residing in the $|F=2\rangle$ state.

The experimental setup is shown schematically in Fig. 3. A beam of sodium atoms was formed by an aperture diaphragm, S_1, 0.14 mm in diameter, mounted on the atomic source, and a collimating slit diaphragm, S_2, with a vertical dimension of $h=0.5$ mm and 0.24 mm wide, spaced at a distance of $l_1 = 250$ mm. Inserted vertically into the atomic beam at a distance of $l_2 = 33$ mm from the collimating diaphragm was a quartz plate with a length of $L=25$ mm. The plate was 0.5 mm thick, and its entrance and exit faces were beveled at an angle of 45°, this making it possible to bring in a laser beam at the same angle. While reflecting repeatedly inside the plate, the laser beam produced an evanescent wave. The radiation power in the laser beam at the entrance to the plate was $P=40$ mW. The Rabi frequency in the evanescent wave was in that case $\Omega_R(0)/2\pi = (P\beta^2/n\pi w_x w_y I_{sat})^{1/2}(\Gamma/2\pi) = 480$ MHz, where $I_{sat} = 6$ mW/cm^2 is the transition saturation intensity, $\Gamma/2\pi$ is the homogeneous transition width, and $\beta^2 = 6.9$ is the Fresnel coefficient [20] relating together the field intensity in the evanescent wave and that inside the plate with a refractive index of $n=1.45$ at an angle of

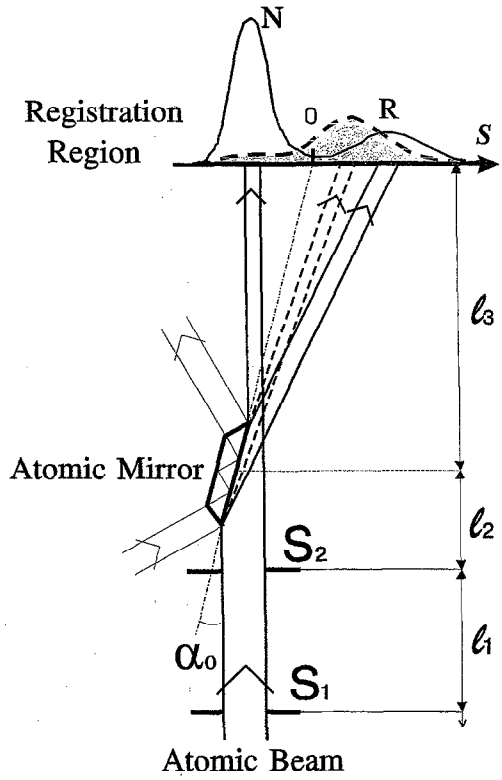

Fig. 3. Schematic diagram of the experimental setup. The atomic beam formed by two diaphragms reflects from the atomic mirror. In the detection region, the beam of the probe laser scans the cross section of the atomic beam in the direction S. The peak N corresponds to that part of the incident atomic beam which has passed by the atomic mirror, and the peak R indicates the position of the reflected beam. The dashed profile shows the position of the atomic beam cooled in the evanescent light wave. α_0 is the inclination angle of the atomic mirror relative to the incident atomic beam.

incidence of $\theta = 45°$ in the case of field polarization parallel to the plane of incidence. The Gaussian beam waists were $w_x = 0.74$ mm and $w_y = 0.53$ mm.

The spatial distribution of the atomic beam reflected from the evanescent light wave was probed by measuring the fluorescence signal excited by the probe laser beam at a distance of $l_3 = 322$ mm from the center of the plate. The probe laser beam focused into a spot measuring 5 mm along the atomic beam and 0.1 mm across intersected the latter at an angle of 73°. The atomic beam profile was measured by making the laser beam scan the atomic beam horizontally in a direction normal to it. The narrow linewidth of the probe laser (< 10 MHz) made it possible to tune its frequency within the Doppler profile of the absorption line of the atomic beam and thus affect the velocity-selective excitation of the atoms. The fluorescence signal was detected by means of a photomultiplier. This method also enabled us to detect selectively atoms residing either at the $|F = 1\rangle$ or $|F = 2\rangle$ sublevel of the ground state.

To observe the cooling of the atoms, the frequency of the evanescent light wave was made higher than that of the atomic transition $|F = 1\rangle \rightarrow |e\rangle$ by an amount of $\delta/2\pi = (\omega - (\omega_1 + k_x v))/2\pi$ (see Fig. 2a). All the atoms incident upon the evanescent wave were preliminarily raised to the sublevel $|F = 1\rangle$ by using some of the probe laser radiation. The reflected atoms were detected at the $|F = 2\rangle$ sublevel, for it was exactly these atoms that had undergone the spontaneous decay $|1, n\rangle \rightarrow |2, n-1\rangle$ and lost some of their kinetic energy.

To affect the specular reflection of the atoms, the frequency of the evanescent wave was detuned by an amount of $\delta_2/2\pi = (\omega - (\omega_2 + k_x v))/2\pi$ (see Fig. 2a) from the frequency of the transition $|F = 2\rangle \rightarrow |e\rangle$. The atoms were detected at the $|F = 2\rangle$ sublevel. In that case, it was only those atoms which had initially resided at the $|F = 2\rangle$ sublevel and reflected elastically from the atomic mirror that were detected.

That part of the initial atomic beam that had passed by the quartz plate (Fig. 3) served to determine the zero point in the detection region. The angle of reflection α was determined from the center of the peak of reflected atoms. The accuracy of such a determination was estimated at 0.1 mrad. The reflection coefficient ρ of the atomic mirror was found from the surface area of the peak of reflected atoms.

4. Results and discussion

4.1. Reflection cooling at various frequency detunings of the evanescent wave

Fig. 4 presents profiles of the atomic beam reflected from the atomic mirror, obtained with different values of the evanescent wave frequency detuning δ. The inclination angle α_0 of the atomic mirror amounted to 1.4 mrad. The maximum Rabi frequency in the evanescent wave was $\Omega_R(0)/2\pi = 480$ MHz. The velocity of the atoms detected was $v = 650$ m/s.

Each of the atomic beam profiles presented consists of two peaks. The right-hand peak (we will call it the cooled beam) corresponds to the reflected part of the atomic beam whose atoms experienced in the course of reflection the decay to the state $|F = 2, n-1\rangle$ in the evanescent wave (see Fig. 2b). The left-hand peak corresponds to that part of the initial atomic beam that had passed by the quartz plate (Fig. 3). Since all the atoms were pumped to the sublevel $|F = 1\rangle$ prior to their interaction with the evanescent wave, the presence of the left-hand peak is explained by the fact that some atoms were pumped to the sublevel $|F = 2\rangle$ by the scattered light from the evanescent wave, whose wave vector is directed along the beam. That this is

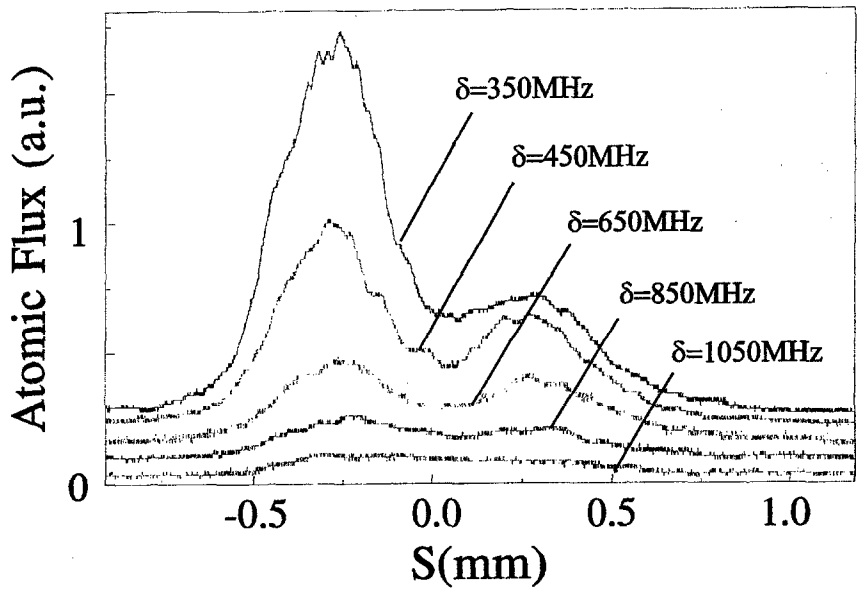

Fig. 4. Beam profiles of cooled atoms for various evanescent wave frequency detuning values.

true is also confirmed by the fact that the relationship between the height of the peak and the frequency detuning δ of the evanescent wave is of Lorentzian character. Note that this light is in resonance with the atoms residing at the sublevel $|F=1\rangle$ and does not interact with the cooled atoms that have already moved to the sublevel $|F=2\rangle$. Thus, it has no effect on the right-hand peak of the cooled atoms.

As the frequency detuning of the evanescent wave is increased, the peak of cooled atoms shifts towards greater angles, which means that the amount energy withdrawn from the atoms in the course of reflection decreases, this being in full agreement with the theory (see formula (10)). In the case of elastic, specular reflection, the angle of reflection is a maximum and is equal to the angle of incidence. As δ is increased, the probability of spontaneous atomic decay to the upper sublevel $|F=2\rangle$ becomes lower (see formula (11)), this resulting in a decrease in the reflected beam intensity. Thus, the efficiency of reflection cooling decreases noticeably with increasing frequency detuning. In the given experimental geometry, the most efficient atomic beam cooling was achieved in the frequency detuning range 300–400 MHz.

As the frequency detuning was reduced to fall within the region $\delta < 300$ MHz, the cooling effect was observed to vanish, and side effects associated with the resonance deflection of the atoms by the scattered laser light became manifest. Lowering the frequency detuning increases the saturation of the atomic transition, and the cooling of the atoms in the evanescent wave becomes less effective for the following two reasons. First, with the transition becoming more saturated, the atoms, on average, undergo the decay $|1, n\rangle \rightarrow |2, n-1\rangle$ at greater distances from the surface, where the optical potential difference

$$\Delta U = U_1(z) - U_2(z) \approx (2/3)\left[\hbar\Omega_R^2(0)/\delta\right] \times \left[\delta_{hfs}/(\delta+\delta_{hfs})\right]\exp(-z/\Lambda) \quad (12)$$

decreases, reducing the amount of energy withdrawn from the atoms. Secondly, the rise of the atomic excitation probability at a small frequency detuning increases the heating of the atoms on account of transitions to the attractive state $|3, n-1\rangle$.

4.2. Reflection cooling at various evanescent wave intensities

Reflection cooling by its nature must be independent of the intensity of the evanescent wave. The trajectory of an atom in reflection is governed by its initial velocity and angle of incidence upon the atomic mirror. A change in the evanescent wave intensity only causes the atomic trajectory to be translated relative to the dielectric–vacuum interface. If threshold condition (8) is satisfied, the atom will reflect from the evanescent wave either elastically or inelastically, depending on whether it has suffered a spontaneous decay or not. As the evanescent wave intensity is reduced, condition (8) ceases to be satisfied, primarily for those atoms in the incident beam (having a finite divergence) which have had the greatest angle of incidence. Such atoms fall on the surface of the quartz plate and leave the beam. This leads to a reduction of the intensity of the reflected beam and a displacement of the center of the beam profile being detected towards smaller angles. And it was exactly such behavior of the reflected atoms that we

observed experimentally when changing the intensity of the evanescent wave.

When measuring the reflection of the atoms as a function of the evanescent wave intensity, the atomic mirror was set to the edge of the incident atomic beam and inclined at a slightly greater angle, $\alpha_0 = 1.55$ mrad, so that that part of the beam which passed by the mirror was largely suppressed. The velocity of the atoms being detected was $v = 650$ m/s. Presented in Fig. 5 are series of profiles of the cooled (1c–5c) and mirror-reflected (1s–5s) atomic beams, obtained with different evanescent wave intensities and constant frequency detuning values, $\delta/2\pi = 350$ MHz and $\delta_2/2\pi = 650$ MHz, respectively. The high frequency detuning value of 650 MHz ensures the specular character of atomic reflection, and the low one, 350 MHz, provides for the efficient cooling of the atoms. The profiles of the 1s–5s series consist of two peaks, the left-hand peak corresponding to the position of the control atomic beam and the right-hand one, the position of the mirror-reflected beam. In the 1c–5c series, each profile features a single peak corresponding to the beam of atoms that have suffered undergone reflection.

The profiles 1c and 1s were obtained at the maximum Rabi frequency of $\Omega_R(0)/2\pi = 460$ MHz. Each next pair of profiles corresponds to a lower Rabi frequency value.

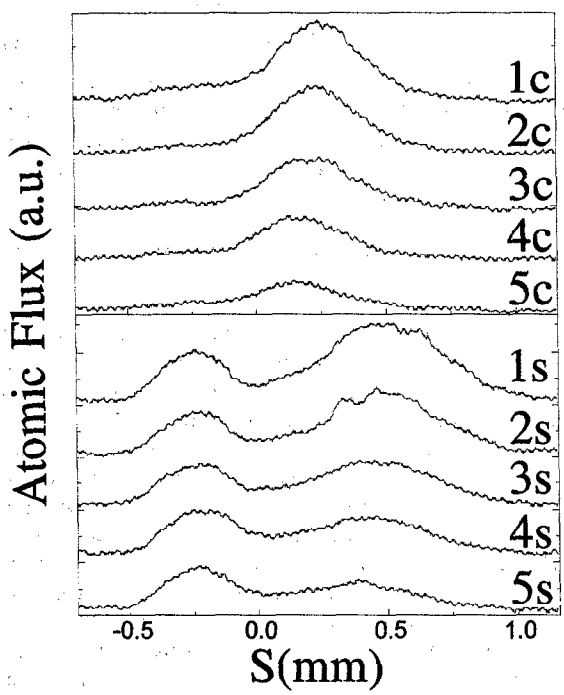

Fig. 5. Atomic beam profiles for various evanescent wave intensity values. Top – beam profiles for cooled atoms; bottom – beam profiles in the case of specular reflection. The Rabi frequency $\Omega_R(0)/2\pi$: 1c,s – 380 MHz; 2 – 343 MHz; 3 – 320 MHz; 4 – 287 MHz; 5 – 258 MHz.

One can see from the figure that the intensity of the beam of reflected atoms drops as the evanescent wave intensity is reduced. The character of this drop in the case of elastic and inelastic reflection remains qualitatively the same, which also agrees with the hypothesis as to the mechanism governing the reduction of the number of reflected atoms due to the violation of reflection condition (8).

In the experiment, we observed a greater loss of atoms in the reflected beam than could be expected for the potential barriers $U_1(0)$ and $U_2(0)$. To illustrate, the actual barrier height in the case of specular reflection was 20% less than the maximum light-induced shift of the $|F = 2\rangle$ sublevel with the frequency detuning $\delta_2/2\pi = 650$ MHz. We associate the lowering of the potential barrier with the following two factors. The first is the attraction of the atoms to the surface of the quartz plate by the Van der Waals forces, which becomes important at distances of some 50 nm from the plate. The second factor is the surface roughness of the plate. All the factors influencing the formation of the reflected atomic beam will be considered in greater detail in Section 5.

4.3. Reflection cooling at optimal evanescent light wave parameters

In the preceding Sections 4.1 and 4.2, we have found the optimal detuning and evanescent light wave intensity parameters for the observation of the reflection cooling effect in our experimental geometry. The most efficient cooling of the atomic beam was achieved with a frequency detuning of $\delta/2\pi = 350$ MHz and a Rabi frequency of $\Omega_R(0)/2\pi = 460$ MHz (profile 2 in Fig. 6).

It should be noted that the whole initial atomic beam was much larger than its part which was incident into the atomic mirror. So the reflected beam was the only observable object in our experiment. We will compare the profile of the cooled atomic beam with that of the specular-reflected beam obtained with the same evanescent light wave intensity and a frequency detuning of $\delta_2/2\pi = 650$ MHz. The specular angle of reflection, determined from the center of the beam profile, was $\alpha_s = 1.53$ mrad.

In comparing profiles 1 and 2, consideration should be given to the fact that when observing the reflection cooling effect, all the atoms in the incident beam were pumped to the $|F = 1\rangle$ sublevel. When observing specular reflection, the atoms in the incident beam populated both ground state sublevels. The choice of the frequency detuning $\delta_2/2\pi =$ 650 MHz for the observation of specular reflection practically excluded the possibility of detecting the atoms that initially populated the $|F = 1\rangle$. The probability that such atoms would be pumped to the sublevel being detected and reflect from the atomic mirror was no more than 1%. Thus, the mirror-reflected atomic beam was formed by the atoms initially populating the $|F = 2\rangle$ sublevel. The proportion of such atoms in the incident thermal beam was equal to

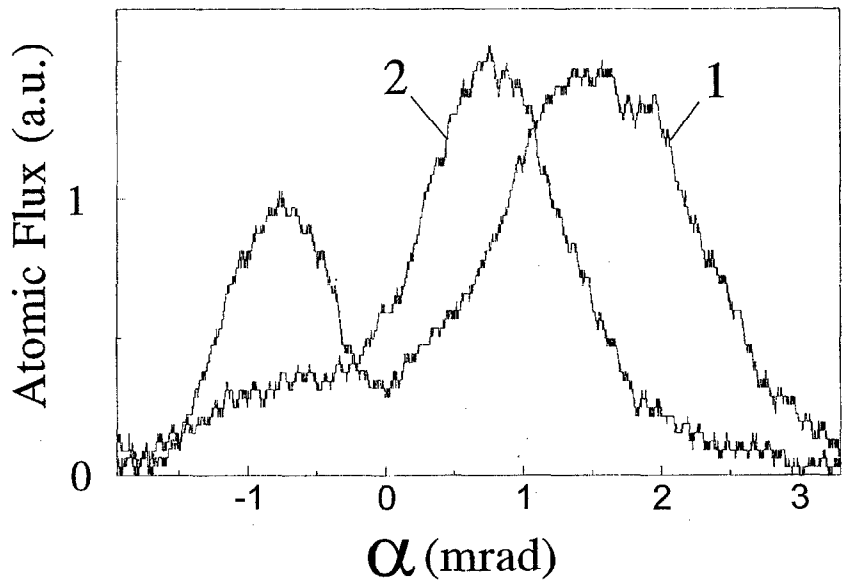

Fig. 6. Experimental atomic beam profiles: 1 – beam profile in the case of specular reflection; 2 – beam profile of cooled atoms.

5/8. Now we can estimate the relative amount of atoms that had cooled on reflection from the evanescent light wave: $\rho_{\mathrm{cool,exp}} = N_{\mathrm{cool}}/N_{\mathrm{spec}} \approx (5/8)(S_{\mathrm{cool}}/S_{\mathrm{spec}}) = 0.5$, where S_{cool} and S_{spec} are the areas of the peaks of the cooled and specular-reflected atomic beams, respectively. We have also carried out the computer simulation of the inelastic atomic reflection process, which has showed that the probability p_{12} of the spontaneous $|F=1\rangle \rightarrow |F=2\rangle$ transition (the very transition providing for the cooling of the atoms) in the evanescent light wave comes to 0.64. The reflection coefficient $\rho_{\mathrm{cool,theor}}$ is in that case equal to 0.53. The difference between the reflection coefficient ρ_{cool} and the probability p_{12} of the $|F=1\rangle \rightarrow |F=2\rangle$ transition is explained by the fact that in the course of reflection those atoms which made the transition at great distances from the atomic mirror where the barrier height of U_2 proved insufficient for their reflection were lost.

The average angle of reflection of the cooled atoms, α_c, determined from the center of the recorded atomic beam profile amounted to 0.8 mrad. Thus, the transverse momentum component of the atoms was reduced almost by half. It should be noted that it was the hottest atoms that were lost in reflection. As already discussed earlier, this causes the peak of reflected atoms to shift towards smaller angles. This effect can rigorously be accounted for by using Monte-Carlo simulation (see Section 5).

In addition to the fact that the beam of cooled atoms reflects from the atomic mirror at a smaller angle, it also has a smaller divergence that the beam of specular-reflected atoms. Those atoms which fall upon the atomic mirror at greater angles penetrate deeper into the evanescent wave and hence lose more energy. In the low saturation approximation, where the probability of spontaneous decay on reflection is much lower than unity, one can demonstrate that the loss of energy by the cooled atoms is, on the average, proportional to their initial energy [13]. In our case, the divergence of the beam of cooled atoms was measured to be smaller by a factor of some 1.5 than that of the specular-reflected beam. Thus, we can also speak of the reduction of the transverse temperature of the atoms in the beam in the course of its inelastic reflection from the evanescent light wave. In our case, this reduction amounted to 2.25 times.

The tangential dipole force component $F_{\mathrm{dip},x}$ has a noticeable effect on the angular distribution of the reflected beam. Insofar as the evanescent light wave in the quartz plate was produced by multiple reflection of a focused Gaussian beam, the reflecting surface had the form of a series of bright spots. Each spot defocused the atomic beam. The local radius of curvature of such a mirror in the x–z plane was $R \sim w_x^2/(\Lambda \ln 2)$. As a result of defocusing, the reflected beam acquired an additional divergence of about 0.6 mrad.

5. Monte-Carlo simulation

In this section, we will consider the computer simulation of the reflection of atoms from an evanescent light wave and compare the computation results with the experimental results. The reflection process was simulated by computing atomic trajectories in the evanescent light wave field using the Monte-Carlo method. The atoms are taken to be well localized because their extent, if they are regarded as wave packets, is small compared to the characteristic length Λ of the evanescent wave. The effects of

fluctuations of the dipole force, the spontaneous force (i.e., the photon recoil), and the defocusing due to the Gaussian profile of the laser beam are included. By comparing the experimental results with the model predictions, one can assess the importance of these effects. First we will outline the Monte-Carlo simulation.

Consider an atom at the lower ground state sublevel $|F=1\rangle$, which enters the field of an evanescent light wave. In the case of positive frequency detuning of the light field, the atom adiabatically gets into the state $|1, n\rangle$ and experiences the action of the repulsive potential $U_1(r)$ (see Fig. 2). As the atom penetrates deeper into the evanescent light wave field, the probability that it will spontaneously emit radiation becomes higher. If such a spontaneous emission occurs, the atom suffers a recoil and may move to one of the dressed states $|1, n-1\rangle$, $|2, n-1\rangle$, or $|3, n-2\rangle$. Having made the transition to the state $|1, n-1\rangle$, the atom will continue its motion along a specular reflection trajectory. The overall effect from such transitions causes the atomic momentum to fluctuate. If after emitting a spontaneous photon the atom finds itself in the state $|2, n-1\rangle$, it will no more suffer spontaneous decays, thanks to the large frequency detuning $\delta+\delta_{\mathrm{hfs}}$. Let such a spontaneous decay take place at the point $r_{1\to 2}$. From that point onwards, the trajectory of the atom will be governed by the repulsive potential $U_2(r)$. Such an atom will fly out of the light field while residing at the $|F=2\rangle$ sublevel and having lost some of its kinetic energy, $U_1(r_{1\to 2})-U_2(r_{1\to 2})$. The transition to the attractive state $|3, n-2\rangle$ brings about different consequences, depending on the direction of the atomic motion in the evanescent light wave. If such a transition occurs while the atom moves toward the surface, the atom will then accelerate. If the transition takes place while the atom moves away from the surface, having already passed the turning point, it will, on the contrary, be retarded in the attractive potential. Such transitions, on average, lead to an increase of the divergence of the reflected beam. The atomic velocity fluctuations due to transitions to the attractive state are small because of the short lifetime ($\sim 1/\Gamma$) of this state and are of the order of a few recoil momenta.

The trajectory of an atom reflecting from the evanescent wave was calculated by integrating the equation of motion

$$M\dot{v} = -\nabla U_i, \tag{13}$$

where v is the atomic velocity and $i=1, 2, 3$ is the eigenvalue of the dressed state populated at the time t. If the trajectory of an atom penetrated into the region $z<z_{\mathrm{cr}}$, the atom would then be scattered by the surface irregularities of the quartz plate and would be put out of consideration. We estimated the critical distance z_{cr} for the given plate at 50 nm. At each trajectory integration step, the spontaneous emission probability was compared with a random variable $0<\xi<1$. If such a spontaneous emission event did occur, the potential gradient would become that of the new dressed state, and the atomic velocity would be adjusted to account for the recoil. The divergence of the incident atomic beam was governed by the geometry of the experiment and amounted to 0.7 mrad. The reflection-cooled atomic beam was formed by those atoms which had made the $|1, n\rangle \to |2, n-1\rangle$ transition and managed to reflect. The ratio between the number of reflected atoms and the initial number of atoms determined the reflection coefficient ρ. The average angle of reflection of the cooled atoms, α_c, was calculated from the center of gravity of the beam.

When modeling the specular reflection of the atoms, it was only the atoms residing at the $|F=2\rangle$ sublevel that were considered. Those atoms which were pumped in the course of reflection to the other sublevel of the ground state were excluded from consideration because it was only the atoms at the $|F=2\rangle$ sublevel that were detected in the specular refection experiment. The coefficient ρ and the angle α_s for the specular-reflected atoms were determined as described above.

Fig. 7 presents experimental and theoretical relationships between the angle of reflection α_c of the beam of cooled atoms and reflection coefficient ρ on the one hand and the frequency detuning of the evanescent light wave on the other. One can see that the Monte-Carlo simulation results agree well enough with the experimental data. As already discussed above, the efficiency of reflection cooling drops with increasing frequency detuning. This is evidenced by the increase of the angle of reflection and the reduction of the number of reflected atoms. The saturation of the $\alpha_c(\delta)$ curve at high frequency detuning values is explained by the loss of the hottest atoms in reflection. This loss grows rapidly as the frequency detuning is increased, for the barrier height lowers.

Fig. 8 shows the angle of reflection, α, and the reflection coefficient ρ as a function of the evanescent light wave intensity for two reflection modes: reflection cooling

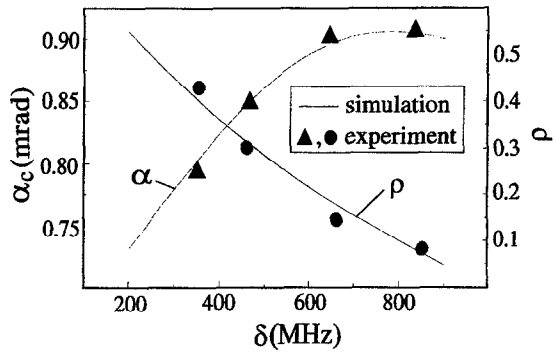

Fig. 7. Angle of reflection, α_c, and the reflection coefficient ρ of the beam of cooled atoms as a function of the frequency detuning of the evanescent wave. See the text for the definition of the coefficient ρ.

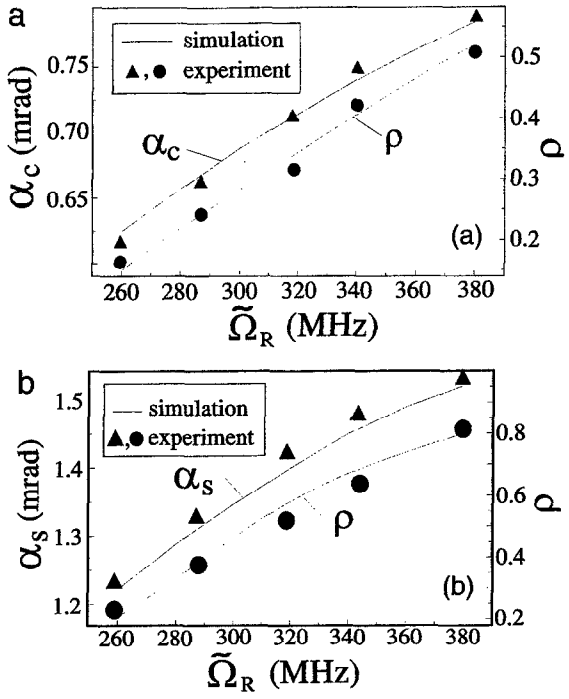

Fig. 8. (a) Angle of reflection, α_c, and the reflection coefficient ρ of the beam of cooled atoms as a function of the Rabi frequency of the evanescent wave. (b) Angle of reflection, α_c, and the reflection coefficient ρ of the atomic beam as a function of the Rabi frequency of the evanescent wave in the case of specular reflection.

(c) and specular reflection (s). The Rabi frequency $\tilde{\Omega}_R = \langle \Omega_R(z_{cr}) \rangle_{x,y}$ determining the barrier height was taken to serve as a quantity characterizing the evanescent light wave intensity. The symbol $\langle \rangle_{x,y}$ denotes the averaging over the x-, y-coordinates in the region occupied by the atomic beam. As the barrier height lowers, the loss of the hottest atoms increases, and the center of the reflected beam shifts towards smaller angles. It should be noted that this additional cooling mechanism had a considerable effect on the angle of reflection of the atomic beam. The numerical modeling of the reflection cooling process at $\tilde{\Omega}_R/2\pi = 500$ MHz, when the loss of atoms in reflection amounted to 2%, yielded $\alpha_c = 0.95$ mrad.

The computer simulation of the process enabled us to estimate the effect of various factors on the angular divergence of the reflected atomic beam. The increase of the beam divergence due to spontaneous emission of radiation came to 0.2 mrad, which is much smaller than that observed experimentally. The main contribution to the additional divergence of the atomic beam was from the defocusing effect. The numerical modeling of the reflection process without the spontaneous emission of radiation yielded 1.3 mrad for the final atomic beam divergence value. This result was obtained for $\tilde{\Omega}_R/2\pi = 500$ MHz, when the loss of atoms in specular reflection was less than 1%. The defocusing of the atomic beam increased its divergence by 0.6 mrad.

An important property of the defocusing effect was its dependence on the angle of incidence of the beam. To illustrate, the atoms incident at smaller angles interacted with a greater number of evanescent light wave nodes and diverged after reflection in a shorter interval of angles. As a result, the center of gravity of the reflected beam shifted a little towards the region of smaller angles. The amount of this shift was found in the computer modeling of the reflection cooling effect to be of the order of 0.05 mrad.

We also modeled the experiment for the case of an ideal atomic mirror where the tangential component of the dipole force is equal to zero and condition (8) is satisfied for all the atoms in the incident beam. All the remaining parameters corresponded to the experimental ones (see Fig. 6). In that case, the angle of reflection of the cooled atomic beam amounted to 1.03 mrad, its final divergence being 0.5 mrad. With the defocusing of the atomic beam and loss of the hottest atoms allowed for, the center of the peak of reflected atoms shifted 0.2 mrad towards smaller angles, and the atomic beam acquired an additional divergence of 0.4 mrad. Considering the error in determining the center of the experimental reflected atomic beam profile, the computer modeling results are in good agreement with the experimental data.

6. Conclusion

Presented in this work are the results of experimental studies into the cooling of a thermal beam of sodium atoms on its reflection from an evanescent light wave. The Sisyphus cooling in the evanescent wave is associated with spontaneous transitions of the atoms between the hyperfine-structure sublevels of their ground state. We have studied the effect of the intensity and frequency detuning of the evanescent wave field on the efficiency of this cooling mechanism.

It is demonstrated that given optimal light field parameters ($\delta \approx \Omega_{R,max}$), one can achieve a two-fold reduction of the transverse momentum component of an atom in a single reflection event, the number of cooled atoms in the reflected beam amounting in that case to more than half their total number.

The use of this evanescent-wave cooling mechanism in the case of repeated reflection of atoms in a trap [13] might enable one to cool them to sub-Doppler temperatures and achieve a high atomic gas density. This makes this cooling method a promising means of affecting the Bose–Einstein condensation.

Acknowledgements

This work was performed with partial support of the Russian Basic Research Foundation, grant 95-02-05350. Yu.B.O. thanks the Alexander von Humboldt Foundation for their support.

References

[1] V.G. Minogin and V.S. Letokhov, Laser Light Pressure on Atoms (Gordon and Breach, New York, 1987).
[2] S. Chu and C. Wieman, eds., Laser Cooling and Trapping of Atoms, J. Opt. Soc. Am. B 6, Special Issue No11, 1989.
[3] T.W. Hansch and A.L. Schavlow, Optics Comm. 13 (1975) 68.
[4] D.J. Wineland and H. Dehmelt, Bull. Am. Phys. Soc. 20 (1975) 637.
[5] V.S. Letokhov, V.G. Minogin and B.D. Pavlik, Zh. Eksp. Teor. Fiz. 72 (1977) 1328 (in Russian) (Engl. transl. Sov. Phys. JETP 45 (1977)) 698.
[6] A.P. Kazantsev, Zh. Eksp. Teor. Fiz. 66 (1974) 1599.
[7] J. Dalibard and C. Cohen-Tannoudji, J. Opt. Soc. Am. B 2 (1985) 1707.
[8] A. Aspect, J. Dalibard, A. Heidmann, C. Salomon and C. Cohen-Tannoudji, Phys. Rev. Lett. 57 (1986) 1688.
[9] J. Dalibard and C. Cohen-Tannoudji, J. Opt. Soc. Am. B 6 (1989) 2023.
[10] R. Gupta, C. Xie, S. Padua, H. Batelaan and H. Metcalf, Phys. Rev. Lett. 71 (1993) 3087.
[11] Yu. Ovchinnikov, J. Söding and R. Grimm, Pis'ma v ZETF 61 (1995) 23 (in Russian); JETP Lett. 61 (1995) 10.
[12] K. Helmerson, S. Rolston, L. Goldner and W. Phillips, Workshop on Optics and Interferometry with Atoms, Insel Reichenau, Germany, June 1992, unpublished.
[13] J. Söding, R. Grimm and Yu.B. Ovchinnikov, Optics Comm. 119 (1995) 652.
[14] Yu. Ovchinnikov, D.V. Laryushin, V.I. Balykin and V.S. Letokhov, Pis'ma v ZETF 62 (1995) 102.
[15] R.J. Cook and R.K. Hill, Optics Comm. 43 (1982) 258.
[16]gjV.I. Balykin, V.S. Letokhov, Yu.B. Ovchinnikov and A.I. Sidorov, Phys. Rev. Lett. 60 (1988) 2137.
[17] M.A. Kasevich, D.S. Weiss and S. Chu, Optics Lett. 15 (1990) 607.
[18] C.G. Aminoff, A.M. Steane, P. Bouyer, P. Desboilles, J. Dalibard and C. Cohen-Tannoudji, Phys. Rev. Lett. 71 (1993) 3083.
[19] W. Seifert, C.S. Adams, V.I. Balykin, C. Heine, Yu. Ovchinnikov and J. Mlynek, Phys. Rev. A 49 (1994) 3814.
[20] M. Born and E. Wolf, Principles of Optics, (Pergamon, Oxford, 1970) p. 47.